Polymer Thin Film Integrated Optics: Fabrication and Characterization of Polystyrene Waveguides

J. T. IVES and W. M. REICHERT,* *Department of Bioengineering, and Center for Sensor Technology, University of Utah, Salt Lake City, Utah 84112*

Synopsis

The fabrication and characterization of 1–3 μm polystyrene thin film integrated optical (IO) waveguides is presented. The polymer films were spun-cast onto quartz and glass microscope slides, yielding waveguides of varying quality. The majority of defects in the polymer films appeared to be introduced during the curing process. Laser light (488 nm) was coupled into the polymer films using the prism coupling technique. The collected Raman emission was used to characterize physical and light guiding properties of acceptable polymer films. The Raman intensity spectra collected as a function of the coupling angle supplied data for the calculation of polymer film thickness and refractive index as well as providing general measure of waveguide suitability. The intensity loss due to scatter of several waveguides was also determined to rigorously evaluate waveguide quality.

INTRODUCTION

The properties associated with polymer thin film waveguides suitable for spectroscopic applications are uniform thickness, good adhesion to the substrate, lack of scattering defects in the polymer film and at the surfaces, and a low fluorescent background. Towards the goal of further defining the thin film integrated optic (IO) spectroscopic technique, in this report we offer a protocol for producing, characterizing, and finally selecting polymer IO waveguides of spectroscopic quality. In a subsequent report we present fluorescent data collected from monolayer structures at the polymer–air and polymer–water interface which attempts to separate evanescent and scatter-excited signal.[1]

Briefly, light propagates down optical waveguides by virtue of repeated total internal reflection back and forth between the two interior surfaces. This mode of light propagation can occur only if the adjacent media are of lower refractive index. In the integrated optical limit, the dimensions of the waveguide become so small that the number of total reflections per unit distance can exceed 500 reflections/cm (approximately 50 times the reflections per cm of a typical ATR crystal). The multitude of crisscrossing, totally reflecting, light rays that exist in the waveguide now overlap to form optical interference patterns. Each of the totally reflected rays that sum to form an interference

*To whom correspondence should be sent.

Journal of Applied Polymer Science, Vol. 36, 429–443 (1988)
© 1988 John Wiley & Sons, Inc. CCC 0021-8995/88/020429-15$04.00

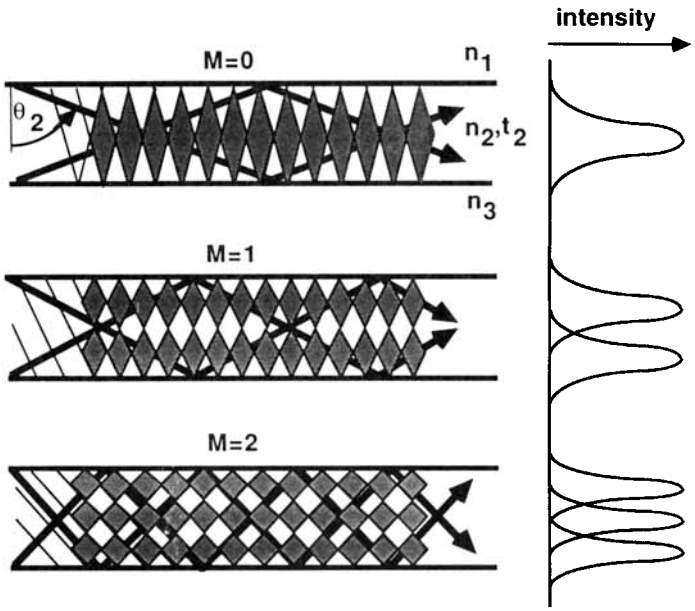

Fig. 1. Intensity distribution across a thin film waveguide for the three lowest order modes. If the angle of total reflection simultaneously satisfies the electromagnetic boundary conditions at both interfaces, then a constructive interference pattern is created. Each antinode of a constructive interference pattern is an intensity maximum of the resulting guided mode intensity distribution.

pattern also produce a local evanescent field at the outer surface of the waveguide. The ray summation process therefore produces a continuous field inside the waveguide as well as a continuous evanescent field at the waveguide surface.[2-4]

For a given combination of superstrate (refractive index n_1), waveguide (refractive index n_2 and thickness t_2), and substrate (refractive index n_3), where $n_1 < n_2 > n_3$ (e.g., air–polymer film–microscope slide), each angle of total reflection, in essence, represents an interference pattern. Only a discrete and finite set of the possible total reflection angles are capable of producing the constructive interference patterns which allow light to travel, with minimum radiation loss, along the waveguide (Fig. 1). These nonradiative interference patterns are called bound or guided modes. Experimental trial has shown the minimum polymer film thickness capable of supporting a single bound mode to be on the order of 1 μm. However, in general, the thicker the waveguide, or the larger the refractive index difference between the film and surrounding media, the greater the number of propagating bound modes supported by the waveguide.

The most common technique for coupling laser light into polymer thin film IO waveguides is evanescent prism coupling.[5] Other techniques such as end fire, taper, and grating coupling are also employed.[6] In prism coupling, an evanescent field is created by totally reflecting the incident laser radiation off the bottom face of a right angle, high index prism (Fig. 2). The angle of the laser light is adjusted until the evanescent field of the totally reflected beam

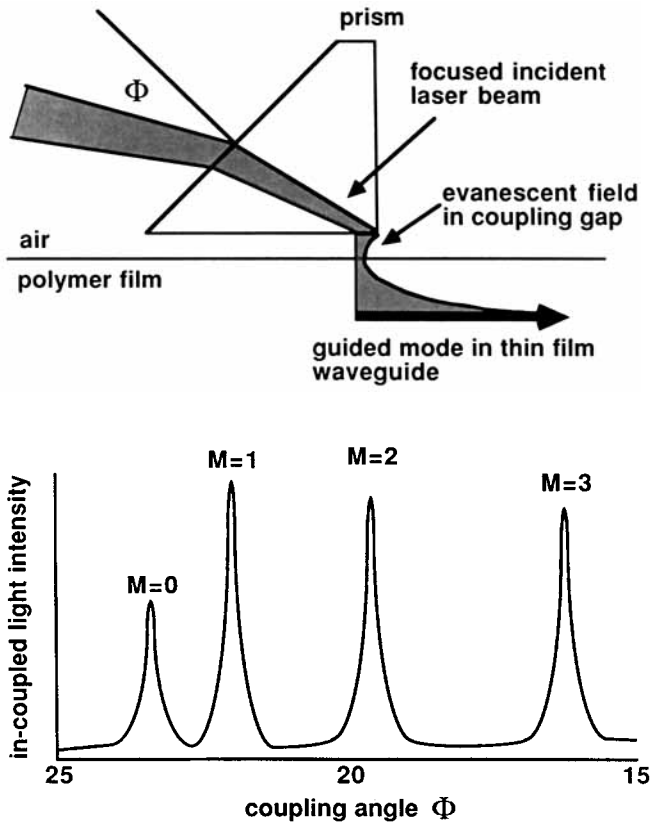

Fig. 2. Prism coupling of light into a thin film waveguide. Light is coupled from the prism to the thin film when the wave vector in the coupling gap matches the evanescent tail of a guided mode structure (top). Only specific coupling angles will satisfy this condition (one discrete range of angles for each mode) and transfer energy to the thin film, as shown in the calculated angular intensity spectrum for a four mode waveguide (bottom).

matches wave vectors with a guided mode. When this matching is achieved, a bright streak of light appears which is confined to the thin film waveguide.

As reviewed by Westwood and Wei,[7] integrated optics has provided an alternative to such techniques as ellipsometry, interferometry, and surface plasmon resonance for determining optical parameters of thin films at interfaces. The first comprehensive application of IO techniques to the analysis of polymer thin films was pursued by Swalen and co-workers.[8,9] In this work, polymer film refractive index, thickness, and optical propagation parameters (optical absorbance and polarization anisotropy) were determined. In the mid-1970s, Levy et al.[10] reported the observation of Raman scattered light from polymer thin film waveguides. Prior to this report the only reliable technique for the collection of vibrational spectra from micron-thick polymer thin films was Fourier transform infrared absorption (FTIR) spectroscopy.[11]

Over the last two decades, prism-coupled thin film IO waveguides have become an established spectroscopic technique. In addition to collecting vibrational spectra from 1–6-μm polymer films, several papers have reported the use of laminate waveguide structures for the observation of Raman

TABLE I
IO Waveguide Spectroscopy of Polymer Thin Films[a]

Waveguide[b]	Spectroscopy/waveguide fabrication
Substrate/polymer film/air	Theory, no experiment[12,13]
Fused silica/PMMA (1–6 μm)/air	Raman of polymer film/DB, SC[10,14]
Pyrex/PS (1 μm)/air	Raman of polymer film/DB, SC[15,16]
Pyrex/PS–napthaline (1–2 μm)/air	Raman of PS–napthaline composite film/DB[17]
PMMA block/PVA (2 μm)/air	Raman of polymer substrate and film/SC[18,19]
Fused silica/PS (1–4 μm)/air	Brillouin scattering of polymer film/HF[20]
Fused silica/PS (2μm)/air	Coherent anti-Stokes Raman of polymer film/SC[21]
Substrate/polymer film/polymer film/air	Theory, no experiment[12]
Pyrex/PMMA (0.5 μm)/PVA (1.5 μm)/air	Raman of laminate/SC[18,19]
Pyrex/PVA (1.5 μm)/PS (0.5 μm)/air	Raman of laminate/SC[18,19,22]
Fused silica/PVP (2.5 μm)/PS (1 μm)/air	Raman of laminate/HF[23]
Pyrex/Corning glass (1 μm)/PS (0.8 μm)/air	Raman of PS overlayer/SP, SC[24]

[a] PMMA = poly(methyl methacrylate); PS = polystyrene; PVA = poly(vinyl alcohol); PVP = poly(vinyl pyrrolidone); DB = doctor blading; SC = spin casting; HF = horizontal flow; SP = sputtering.
[b] All waveguides utilized prism coupled light.

scattering in submicron polymer films which has pushed the sensitivity of the technique to the submicron domain. The use of IO waveguide emission spectroscopy for the characterization of polymer thin films is reviewed in Table I.

EXPERIMENTAL

Secondary standards of polystyrene (M_n = 85,600, Aldrich) were "purified" by a repeated toluene–methanol solvation–precipitation sequence to remove residual monomer. Viscous solutions [10–15% (w/v)] of purified polymer were made in spectrograde chlorobenzene. The polymer solution was applied to acid cleaned quartz or glass microscope slides through 0.5-μm Teflon filters (Schleiker and Scheull). The polymer coated slides were then spun at speeds ranging from 800 to 1100 rpm for periods up to 3–4 min. The waveguides were dried overnight at 60°C and stored in sealed acid cleaned jars until used. Depending on the solution viscosity and spinning velocity, this technique formed 1–3-μm-thick waveguides which support from two to six modes.

Figure 3 shows the optical arrangement used to launch guided modes in the polymer thin film waveguides. A TE polarized 488 nm line from an argon laser was coupled into the polymer films using the high index prism technique. Two $LaSF_5$ prisms (in-coupling and out-coupling) were clamped to the polymer surface using an anodized aluminum support with adjustable rubber lined chucks. The laser beam was focused onto the corner of the coupling prism, and the coupling angle was adjusted until a guided mode was launched (Fig. 2). The coupling angle was precisely selected by attaching the waveguide assembly to an x, y, z stage mounted at the center of rotation of a modified X-ray goniometer (Rigaku). The collection optics were mounted onto the goniometer detector arm for positioning at an angle normal to the waveguide surface. The goniometer has an angular resolution of 0.01° with 360° of rotation available

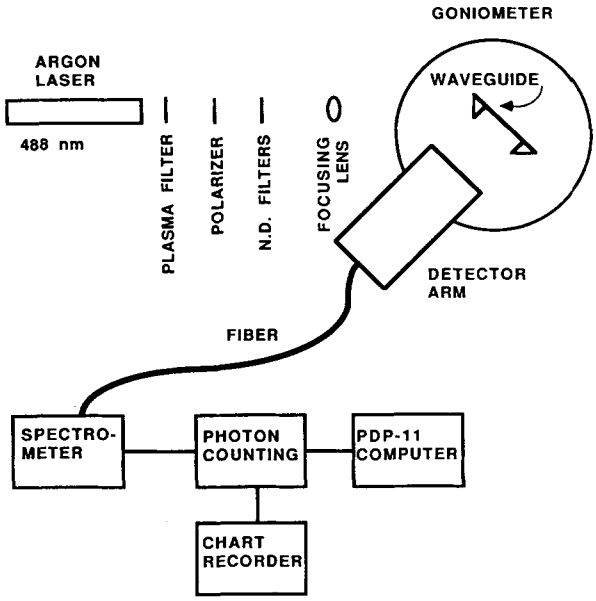

Fig. 3. Schematic of the prism coupling arrangement for launching guided modes in thin polymer films. A fiber or fiber bundle is used with different collection arrangements to deliver the collected light to the spectrometer and photon counting apparatus.

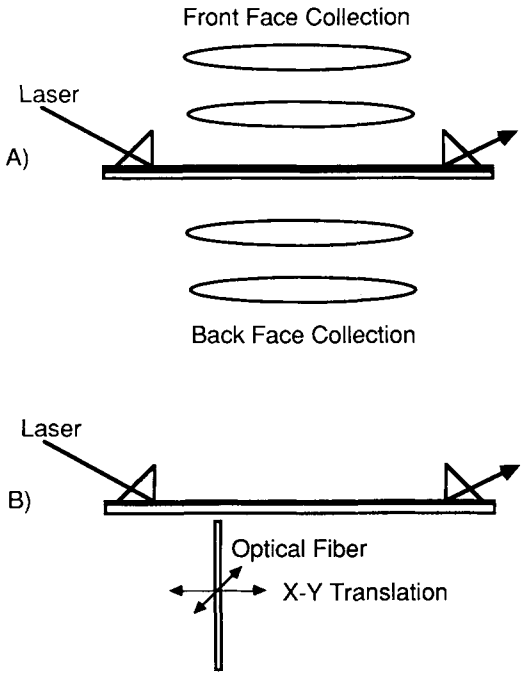

Fig. 4. Two collection arrangements mounted on the detector arm: (A) two lenses collect, collimate, and focus spectral emission onto fiber bundle which delivers light to the spectrometer; (B) spectral emission collected by a single fiber which delivers light directly to the spectrometer.

to both the waveguide mount and the detector arm. This arrangement allowed us to (1) accurately "tune in" individual coupling angles, (2) sweep through the in-coupling angles with a fixed detector position, (3) sweep through the out-coupling angles with a fixed waveguide position, and (4) collect emission with fixed detector and waveguide positions.

Two different collection arrangements could be mounted on the detector arm for use with prism coupled waveguides. The first configuration used lenses for the imaging of emission from the waveguide onto a quartz fiber bundle from either the waveguide surface (front face collection) or through the substrate (back face collection) [Fig. 4(a)]. The lens arrangement was designed for Raman and fluorescence spectroscopy of the waveguide bulk and/or surface.[25] A second more versatile, but less sensitive, configuration used a single fiber to measure the waveguide mode propagation loss and transverse profile [Fig. 4(b)]. The scattered emission was collected using a 200-μm-diameter quartz optical fiber held by a fiber optic positioner on an x–y stage with micrometer drives. The end of the optical fiber was positioned next to the quartz slide surface with the spacing being held constant using a microscope imaging technique. The scattered emission was collected from the approximately 5-cm-long waveguide streak between the in-coupling and out-coupling prisms. Two different spectroscopic signals were used to monitor scatter losses, Rayleigh scatter at 488 nm, and polystyrene Raman scatter at 513 nm. The Raman-scattered emission proved to yield a more reliable indication of waveguide scatter loss than did the Rayleigh-scattered light. All individual data points were obtained by averaging 50 1-s counts from the photon counting system.

RESULTS

Waveguide Fabrication and Coupling Efficiency

As can be seen from Table I, the polymers that most readily form good thin film waveguides in the visible are polystyrene and poly(methyl methacrylate) cast from chlorobenzene, and poly(vinyl alcohol) and poly(vinyl pyrrolidone) cast from water. Polystyrene was selected for this study because (1) it is readily available in reasonably pure, high molecular weight fractions, (2) it has good film forming properties, (3) it lacks significant absorption in the visible wavelengths, and (4) it is not soluble in water and can be immersed in aqueous environments without loss of film quality. In addition to the selection of a proper polymer–solvent system, the properties most closely associated with the production of "good" polymer thin film IO waveguides were (1) use of clean substrates void of scratches and nicks, (2) selection of a casting technique which produces smooth and uniformly thick polymer films void of cracks or bubbles, (3) the lack of scattering sites in the polymer film, (4) a low fluorescence background, and (5) efficient coupling of light into the film.

Scratched or poorly cleaned substrates always resulted in poor waveguides primarily from the introduction of scattering sites at the polymer–substrate interface and poor adhesion of the polymer film to the substrate. Scratched substrates were eliminated through careful handling and the use of new substrates where possible. Clean substrates were obtained by (1) cleaning the

TABLE II
Waveguide Physical Parameters

Spinning rate	μm	Refractive index	Number of modes
800 ≤ rpm < 900	1.94–2.68	1.58–1.60	5–6
800 ≤ rpm < 1000	1.78–2.26	1.58–1.59	4–5
1000 ≤ rpm ≤ 1100	1.05–1.26	1.59–1.60	2–3

quartz slides in hot (80°C) chromic acid for at least 20 min, (2) rinsing the cleaned slides in copious amounts of Millipore water, and (3) using the slides immediately after an overnight drying at 80–100°C (if the slides cannot be used immediately, then they must be stored in acid-cleaned, sealed jars). There appeared to be no difference between quartz or glass slides with respect to the avoidance of scratches or cleaning.

We found the thickness of the film to be a function of spinning rate and solution viscosity. The waveguide thickness, refractive index, and mode number is listed as a function of spinning rate in Table II. The variation in these data was primarily due to the solution viscosity, not the spinning rate. The purification procedure invariably altered the final polymer concentration used for spin casting. This point is, however, not a crucial one because we were not dependent on an empirical recipe for the production of suitable waveguides. The only reliable way to determine waveguide quality is via a subsequent characterization scheme.

The presence of scattering sites in the polymer film significantly reduced the waveguide quality. The most common causes of scattering are dust, bubbles, and microcracks in the polymer film. The source of dust is the ambient environment and is often unavoidable. The presence of scattering sites were minimized by (1) using a nearly monodisperse, high molecular weight polymer fraction (e.g., secondary standard of $M_n \geq 80{,}000$) dissolved in a high boiling point solvent, (2) handling the cleaned quartz slides with forceps or tweezers only, (3) spraying the slides with "dust off" just prior to the application of the polymer solution, (4) filtering solutions through a 0.5-μm filter as it is being applied to the quartz slide to remove unsolvated gel particles, (5) covering the uncured polymer films to minimize exposure to ambient particulates (e.g., place slides in acid cleaned petrie dishes immediately after coating process), and (6) storage of the cured polymer films in acid-cleaned, sealed jars. Although vacuum drying is the most effective means of driving off residual solvent, it frequently results in bubble formation. From our experience, oven drying is effective as the final stage of the curing process (e.g., 60°C effectively drives off residual organic solvent after a 12 h period).

When attempting to utilize thin film waveguides as a spectroscopic tool, one must also avoid a high fluorescent background because it obscures low signal levels and it can attenuate the incoupled light intensity as it propagates down the guide. The sources of fluorescence background were the polymer film and the substrate. The substrate fluorescence was avoided by selecting an optical quality glass or quartz. Quartz slides fluoresced the least while glass slides displayed the greatest fluorescence. The polymer fluorescence, on the other hand, was not as easily eliminated, primarily because many polymers have a

fluorescence which results either from the polymer itself or from residual additives used in processing. Techniques for the elimination of polymer fluorescence are photobleaching the polymer film at high laser intensities prior to taking a spectrum or through some sort of purification scheme. If a solvent can be found that dissolves the impurities and precipitates the polymer, then reprecipitation can be very effective. In general, the toluene–methanol solvation–precipatation technique worked nicely for the reduction of the polystyrene fluorescence due to residual monomer. However, one must keep in mind that exposure of the polymer to a nonpure solvent may simply have the effect of increasing the contamination level.

Presented with a waveguide of sufficient quality, good coupling is only obtained through experience. In our opinion, such tricks as coupling fluids had no significant effect. The only offered suggestions are (1) wiping the coupling prisms with spectral grade solvent (e.g., acetone) soaked lens paper prior to coupling, (2) blow the polymer surface with "dust off" prior to placement of the prisms, (3) line the coupling chucks with thin (1 mm) rubber pads to more uniformly distribute the pressure along the coupling edge of the prism (this modification also has the effect of minimizing prism corner chipping), and (4)

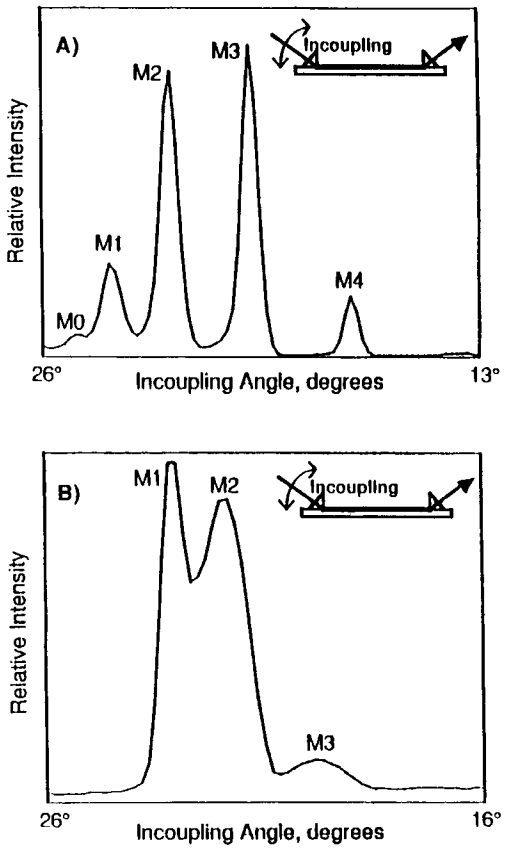

Fig. 5. Angular intensity spectrum of in-coupled waveguide intensity vs. incoupling angle for a "good" waveguide (top) and a "bad" waveguide (bottom).

perform the coupling under a good light source (e.g., fluorescent room lights) such that you can observe the refracted patch at the prism base, indicative of good coupling.

Waveguide Characterization

The Rayleigh and Raman scattered emission collected from a waveguide as a function of location (either longitudinal or transverse) yielded distinctly different results. The Rayleigh emission showed intensity spikes which, in most cases, were entirely absent in the Raman scatter emission. For this reason, in agreement with Bohn and co-workers,[13] we found that Rayleigh scattered light from the waveguide was far too sensitive to minute imperfections in the polymer film to yield a reliable indication of intensity decay along the guide, while the Raman emission was much better suited for this purpose.[26]

The angular intensity spectrum (Raman emission intensity from the waveguide as a function of coupling angle) provided the data for the calculation of waveguide thickness and refractive index (Table II) using a modification of the technique of Swalen et al.[8,9] The waveguide thickness and refractive index may, in turn, be used to calculate the cross-sectional waveguide intensity

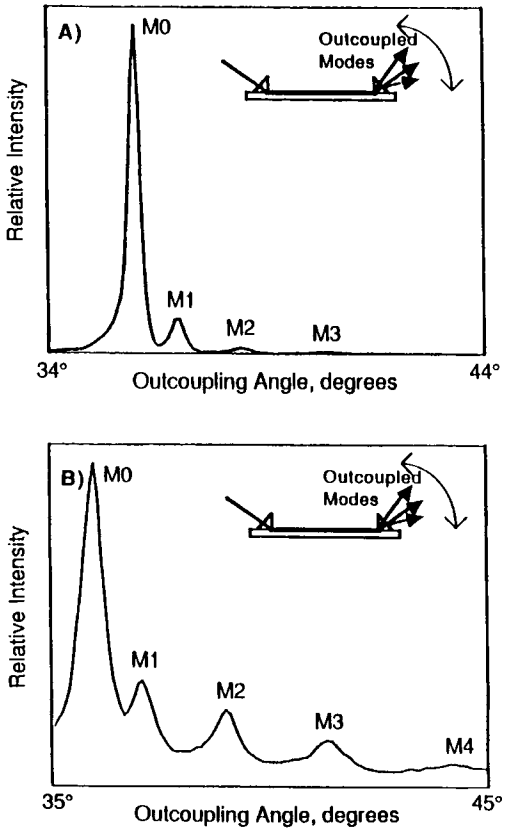

Fig. 6. Angular intensity spectrum of out-coupled waveguide intensity vs. outcoupling angle for a "good" waveguide (top) and a "bad" waveguide (bottom).

patterns for each of the modes supported by the waveguide. FORTRAN software which performs both of these calculations was developed in our labs for use on a Macintosh Plus personal computer.[27]

In addition to waveguide thickness and refractive index, the angularly resolved intensity spectra also provided an estimation of the light propagation properties of the waveguides. Figures 5 and 6 compare the angular resolved intensity spectra typical of "good" and "bad" waveguides. The data in Figure 5 was obtained by scanning the in-coupling angles while collecting the scattered emission from the waveguide. The differences in the peak intensities in Figure 5 was the result of performing an angular spectrum with a right angle prism which yielded different in-coupling efficiencies for each mode. Figure 6 is an angular scan of the out-coupled M lines for two waveguides tuned into the $M = 0$ mode. A smooth, homogeneous waveguide will exhibit sharp intensity peaks at the proper in-coupling angles [Fig. 5(a)] and will also have minimal intermodal cross-coupling at the out-coupling prism [Fig. 6(a)]. A nonuniform waveguide with a large degree of scattering has broadened and/or smeared together in-coupled intensity peaks [Fig. 5(b)] as well as a high degree of intermodal cross-coupling [Fig. 6(b)].

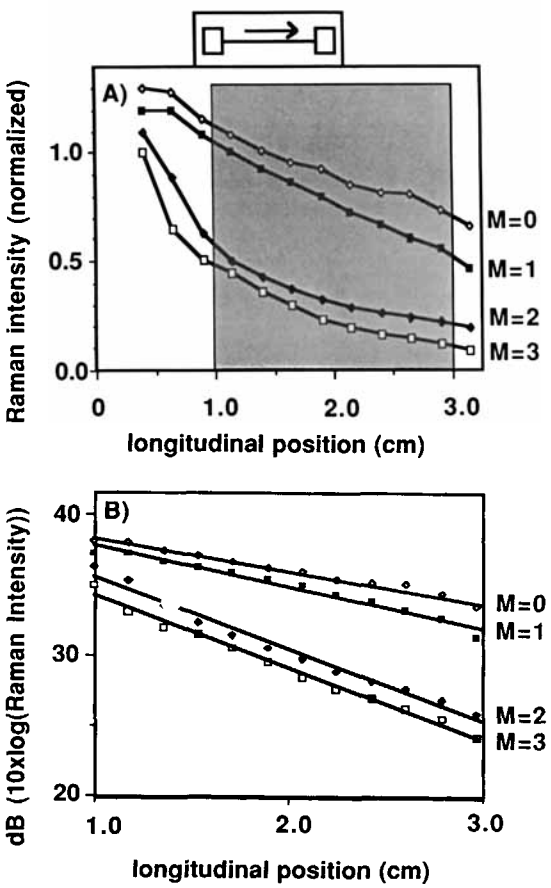

Fig. 7. Longitudinal Raman scatter for four mode waveguide collected using the fiber technique. Only the darkened region of the intensity decay (A) was plotted in terms of dB loss (B).

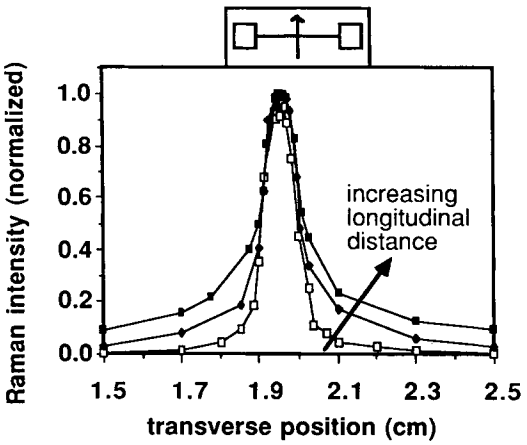

Fig. 8. Transverse Raman scatter profile for $M = 0$ mode of a four-mode waveguide collected at three locations away from the in-coupling prism (1.0, 2.0, and 3.0 cm) using the fiber technique. Note the fanning of the guided mode structure with distance.

Further evaluation of waveguide quality was obtained from waveguide scatter loss measurements. The longitudinal scatter emission yielded the guided mode intensity loss per unit distance (e.g., dB/cm) while the transverse emission yielded the cross-sectional modal intensity profile. Four four-mode waveguides were characterized in this manner. According to the observed angular intensity spectra (Figs. 5 and 6), these four waveguides were

TABLE III
Waveguide Loss

Mode number	dB/cm	$\Delta I/cm \times 100$ (%)
Good waveguide 1 ($t = 2.07\ \mu m$, $n = 1.58$)		
0	−0.91	19
1	−0.59	13
2	−0.82	17
3	−1.14	23
Good waveguide 2 ($t = 1.94\ \mu m$, $n = 1.59$)		
0	−1.57	30
1	−2.05	38
2	−3.65	53
3	−3.62	52
Moderate waveguide ($t = 2.07\ \mu m$, $n = 1.58$)		
0	−2.69	46
1	−3.06	51
2	−3.86	59
3	−9.83	87
Bad waveguide ($t = 2.68\ \mu m$, $n = 1.59$)		
0	−5.73	73
1	−6.08	75
2	NA	NA
3	NA	NA

initially judged to be of three categories, two having good light guiding properties, one of moderate quality and one that was obviously of bad quality.

Figure 7 provides an example of a longitudinal decay spectrum graphed both in terms of normalized intensity [Fig. 7(a)] and dB loss [Fig. 7(b)]. The change in guided mode transverse profile with propagation distance is demonstrated in Figure 8 for the $M = 0$ mode of the same waveguide shown in Figure 7. Transverse data was taken at three different locations away from the coupling prism to observe the change in profile with distance. Table III lists the decay rates of all four waveguides examined, expressed as dB/cm and percent intensity loss per cm distance ($\Delta I/\text{cm} \times 100$).

DISCUSSION

Polymer thin film waveguides are typically cast using one of three techniques: doctor blading, dip coating or horizontal flow, and spin casting. Of those groups who have compared all three techniques,[9,13] the general consensus is that doctor blading and dip coating produce polymer films with uniformity superior to that obtained from spinning. However, the vast majority of thin film waveguides are produced by spin casting because of its comparatively facile mode of production (Table I). The criticisms of spun-cast films are centripitally induced axial anisotropy, the inability to produce quality films thicker than approximately 3 μm, and thinning of the films away from the center of ration.

In our opinion, the use of spun-cast polymer films did not present a problem. The majority of defects seemed to result from the curing process. The formation of bubbles and microcracks seems to be a periodically recurrent problem. Bubbles are usually attributed to entrapped solvent that aggregates and then volatilizes leaving a void or hole in the dried polymer film. Microcracks generally form during the drying process when the volume of the intertwined polymer matrix reduces too quickly as the solvent volatilizes, leaving stress-related cracks much like the cracks found in mud flats. A possible means to reduce these defects is to try a two-step drying procedure. First dry the films at ambient temperatures in the presence of solvent vapor to retard the evaporation process followed by oven drying.

The identification of suitable waveguides was, in essence, a two-step process involving first a cursory visual inspection of the cured polystyrene films, thus discarding those waveguides obviously not suitable for further analysis. The second phase of waveguide selection involved the collection of the angular intensity spectrum (intensity in the waveguide as a function of coupling angle) for each of the remaining waveguides. Only those waveguides exhibiting sharp peaks for the in-coupled light intensity along with a minimal intermodal background were deemed suitable for further use.

The method of identifying waveguides on the basis of quality from the angular intensity spectra seemed to lack sufficient sensitivity to differentiate the best waveguides from the moderately nonlossy guides. This insensitivity results, in part, from the fact that the angular intensity spectra are an indirect measure of waveguide scatter losses. Further analysis using the fiber technique revealed that the two waveguides that exhibited good angular spectra in

Table III actually had losses ranging from −0.59 to −3.62 dB/cm. Therefore, if the waveguides of highest quality are to be identified, one must directly measure the scatter loss of each candidate.

The benchmark figure for a very good polymer thin film waveguide is a loss rate of approximately −1.0 dB/cm. It would appear that only a fraction of the visually acceptable population possessed loss rates of this quality. Although this yield appears low, it must be kept in mind that polymers are naturally strong scatterers of light. The introduction of any additional scattering sites during fabrication will significantly reduce the optical performance of the film. On the other hand, a suitable waveguide which falls into the range of −2.0–4.0 dB/cm is readily identified via the angular intensity spectra. Typically, half of the waveguides fabricated in a given batch were of suitable quality.

The observed decay rates also appeared to be a function of mode number and location along the guide. First of all, the decay rates tended to go up with mode number. This observation makes sense considering the fact that higher order modes have a larger fraction of energy in their evanescent fields and are thus more susceptible to attenuation due to surface defects. The lowest order mode almost invariably exhibited the minimum loss, while, curiously, the second order mode tended to be the most strongly coupled. Second, for a given mode the decay rates tended to be the lowest in the middle 3 cm between the coupling prisms while the decay rates near the coupling prisms varied widely ($-2 >$ dB/cm > -10) with no apparent pattern. A possible explanation for the minimal loss rates is that the middle section was occupied by established

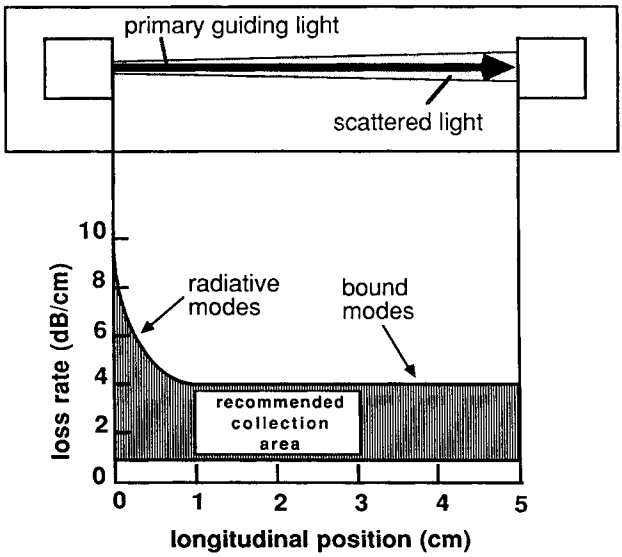

Fig. 9. Mode profile fanning (top) and logitudinal decay (bottom) characteristics of guided modes in polymer films. The rapid decay near the in-coupling prism results from radiative modes which die out rapidly and do not propagate in the midsection of the waveguide. The fanning effect indicates that the guided mode profile deteriorates with distance. Also indicated is the recommended region for spectroscopic collection.

bound modes. Reasons for this erratic behavior near the coupling prisms was attributed to thinning of the polymer film near the ends of the substrate, an unfortunate consequence of spin casting, and the presence of radiative modes near the in-coupling prism. Third, superimposed upon the intensity loss per unit distance was a fanning of the waveguide modal profile as depicted in Figure 8. The fanning effect was believed to result from scattered light that remains trapped as bound modes and laser beam divergence after the focal point at the prism.

These three observations permitted us to, at least figuratively, map the guided mode intensity decay in the approximately 5 cm region between the in-coupling and out-coupling prisms (Fig. 9). From this analysis it appears that the best region for spectroscopic reliability is the second and third centimeter away from the coupling prism. This 2 cm region lacks the radiative modes near the in-coupling prism while also having minimal beam divergence. Our conclusion is presented in contrast to the common practice of collecting spectra near the in-coupling prism because that is the region of highest intensity in the waveguide.

This project was funded by a New Investigator grant from the National Heart, Lung and Blood Institute (HL 32132), a Biomedical Research grant from the Whitaker Foundation, and by a seed grant from the Center for Sensor Technology at the University of Utah. Helpful discussions with D. A. Yoshida, P. A. Suci, D. A. Christensen, and J. D. Andrade at the University of Utah, and J. D. Swalen and J. F. Rabolt of IBM, San Jose are gratefully acknowledged.

References

1. W. M. Reichert and J. T. Ives, to appear.
2. A. W. Snyder and J. D. Love, *Optical Waveguides Theory*, Chapman and Hall, New York, 1983.
3. D. Marcuse, *Theory of Dielectric Waveguides*, Academic, New York, 1974.
4. P. K. Tien, *Rev. Mod. Phys.*, **49**, 361–387 (1977).
5. J. E. Midwinter, *IEEE J. Quant. Electr.*, **QE-6**, 583–590 (1970).
6. P. K. Tien, *Appl. Opt.*, **10**, 2395–2413 (1971).
7. W. D. Westwood and J. S. Wei, *Can. J. Phys.*, **57**, 1247–1259 (1979).
8. J. D. Swalen, M. Tacke, R. Santo, K. F. Reickhoff, and J. Fisher, *Helv. Chim. Acta*, **61**, 960–977 (1978).
9. J. D. Swalen, R. Santo, M. Tacke, and J. Fischer, *IBM J. Res. Dev.*, **21**, 168–175 (1975).
10. Y. Levy, C. I. Imbert, J. Cipiani, S. Racine, and R. Dupeyrat, *Opt. Commun.*, **11**, 66–69 (1974).
11. T. Nguyen, *Prog. Org. Coatings*, **13**, 1–34 (1985).
12. P. W. Bohn, *Anal. Chem.*, **57**, 1203–1208 (1985).
13. D. R. Miller, O. H. Han, and P. W. Bohn, *Appl. Spectrosc.*, **41**, 245–248 (1987).
14. N. E. Schlotter and J. F. Rabolt, *J. Phys. Chem.*, **88**, 2062–2067 (1984).
15. J. F. Rabolt, R. Santo and J. D. Swalen, *Appl. Spectrosc.*, **33**, 549–551 (1979).
16. W. M. Reichert and J. D. Andrade, in *Surface and Interfacial Aspects of Biomedical Polymers: Surface Chemistry and Physics*, J. D. Andrade, Ed., Plenum, New York, 1985, Vol. 1, pp. 421–442.
17. N. E. Schlotter and J. F. Rabolt, *Appl. Spectrosc.*, **38**, 208–211 (1984).
18. J. F. Rabolt, N. E. Schlotter, and J. D. Swalen, *J. Phys. Chem.*, **85**, 4141–4144 (1981).
19. J. F. Rabolt, R. Santo, N. E. Schlotter, and J. D. Swalen, *IBM J. Res. Dev.*, **26**, 209–216 (1982).
20. T. P. Janaky and C. K. Natayanaswamy, *J. Appl. Phys.*, **58**, 2241–2243 (1985).
21. W. M. Hetherington III, N. E. Van Wyck, E. W. Koenig, G. I. Stegeman, and R. M. Fortenberry, *Opt. Lett.*, **9**, 88–89 (1984).

22. J. D. Swalen, N. E. Schlotter, R. Santo, and J. F. Rabolt, *J. Adhesion*, **13**, 189–184 (1981).
23. D. R. Miller, O. H. Han, and P. W. Bohn, *Appl. Spectrosc.*, **41**, 249–255 (1987).
24. J. F. Rabolt, R. Santo, and J. D. Swalen, *Appl. Spectrosc.*, **34**, 517–521 (1980).
25. W. M. Reichert, J. T. Ives, P. A. Suci, and V. Hlady, *Appl. Spectrosc.*, **41**, 636–640 (1987).
26. J. T. Ives, W. M. Reichert, and J. D. Andrade, SPIE, to appear.
27. J. T. Ives and W. M. Reichert, *Comput. Chem.*, (1987), to appear.

Received September 11, 1987
Accepted October 22, 1987